Published in final edited form as:
Curr Opin Struct Biol. 2010 December ; 20(6): 702–710. doi:10.1016/j.sbi.2010.09.005.

A Role for Flexible Loops in Enzyme Catalysis

M. Merced Malabanan, **Tina L. Amyes**, and **John P. Richard***
Department of Chemistry, University at Buffalo, SUNY, Buffalo, NY 14260-3000, USA.

Abstract

Triosephosphate isomerase (TIM), glycerol 3-phosphate dehydrogenase and orotidine 5'-monophosphate decarboxylase each use the binding energy from the interaction of phosphite dianion with a flexible phosphate gripper loop to activate a second, phosphodianion-truncated, substrate towards enzyme-catalyzed proton transfer, hydride transfer and decarboxylation, respectively. Studies on TIM suggest that the most important *general* effect of loop closure over the substrate phosphodianion, and the associated conformational changes, is to extrude water from the enzyme active site. This should cause a decrease in the effective active-site dielectric constant, and an increase in transition state stabilization from enhanced electrostatic interactions with polar amino acid side chains. The most important *specific* effect of these conformational changes is to increase the basicity of the carboxylate side chain of the active site glutamate base by its placement in a “hydrophobic cage”.

Introduction

D. E. Koshland's “induced fit theory” for enzymatic catalysis proposed that formation of the Michaelis complex may be accompanied by conformational changes that bring the catalytic groups at the active site into the proper orientation for catalysis [1]. This imaginative theory was formulated at a time when there was little evidence that protein conformations are, indeed, elastic. It is now common knowledge that substrate-induced conformational changes play several roles in enzymatic catalysis, although only rarely the exact role originally described by Koshland [2,3]. One important conformational change is the closure of *flexible loops* over enzyme-bound substrates, and we present here recent evidence that such loop closure is a key event in catalysis.

Phosphate Gripper Loops

Triosephosphate isomerase (TIM) catalyzes the isomerization of D-glyceraldehyde 3-phosphate (GAP) to give dihydroxyacetone phosphate (DHAP) by a stepwise proton transfer mechanism through an enediolate intermediate (Figure 1A) [4•]. The side chain of Glu-165 (or 167) is the catalytic base that deprotonates the carbon acid substrate [5], the neutral imidazole side chain of His-95 provides electrophilic assistance by polarizing the carbonyl group of enzyme-bound substrate [6], and the cationic side chain of Lys-12 (or 13) [7] interacts favorably with both the substrate phosphodianion group and the developing oxyanion at the enediolate-like transition state [8•].

* To whom correspondence should be addressed. jrichard@buffalo.edu.

The defining feature of catalysis by TIM is the large enzyme conformational changes, most prominently closure of the phosphate gripper loop 6 over the ligand phosphodianion group, observed upon binding of substrate DHAP [9] or intermediate analogs such as 2-phosphoglycolate (PGA) [10] and 2-phosphoglycolohydroxamate (PGH, Figure 1B) [11,12••,13]. The transition state for the TIM-catalyzed isomerization of GAP is stabilized by ca. 12 kcal/mol as a result of interactions between TIM and the substrate phosphodianion group [14], which represents ca. 80% of the total rate acceleration for TIM [14,15]. This large 12 kcal/mol phosphate intrinsic binding energy (IBE) [3] suggests that closure of the phosphate gripper loop 6 and the associated conformational changes make a critical contribution to the enzymatic rate acceleration. The binding of the substrate piece phosphite dianion (HPO_3^{2-}) to TIM results in a 700-fold activation of the enzyme towards proton transfer from the truncated substrate glycolaldehyde, observed as an enzyme-catalyzed deuterium exchange reaction in D_2O [16]. This shows that interactions between TIM and the phosphodianion group of GAP do not simply anchor the whole substrate to TIM, but also serve to activate TIM towards isomerization of the bound substrate [16].

Orotidine 5'-monophosphate (OMP) and DHAP form complexes with orotidine 5'-monophosphate decarboxylase (OMPDC) [18] and glycerol 3-phosphate dehydrogenase (GPDH) [19], respectively, which are also stabilized by interactions with phosphate gripper loops that close over the bound substrate and sequester it from solvent. Phosphate IBEs of 11 - 12 kcal/mol were determined for both the decarboxylation reaction catalyzed by OMPDC (Figure 2A) and the hydride transfer reaction catalyzed by GPDH (Figure 2B) from the ratio of the second-order rate constants for the enzyme-catalyzed reactions of natural and truncated substrates (Chart 1) [20••,21]. The reactions of the truncated substrates catalyzed by TIM, OMPDC and GPDH are all strongly activated by added phosphite dianion (HPO_3^{2-}), and the observed phosphite activation gives phosphite IBEs of 6 - 8 kcal/mol (Chart 1). The difference between the phosphate (ca. 12 kcal/mol) and phosphite (6 - 8 kcal/mol) IBEs represents the entropic advantage of covalent tethering of the oxydianion activator to the truncated substrate [22]. The strong activation and apparent high affinity of the transition states of these enzymatic reactions for HPO_3^{2-} is striking, because these enzymes exhibit low ($K_d \geq 40$ mM) affinities for HPO_3^{2-} in the ground state. Moreover, the similar phosphate/phosphite IBEs determined for three very different enzymatic reactions suggest that this represents an upper limit for the rate acceleration that can be obtained by attaching a phosphodianion group to a small organic substrate [23].

Dynamics of Loop Closure

The activation of TIM, OMPDC and GPDH by HPO_3^{2-} was not predicted from inspection of the numerous X-ray crystal structures that have been determined for these enzymes, but rather was detected in experiments to test the hypothesis that phosphodianion binding interactions make a critical contribution to the rate acceleration for enzymes that utilize a phosphate gripper loop. However, as discussed here, a combined analysis of static X-ray crystal structures and the results of dynamic NMR and fluorescence spectroscopic studies of protein structure provide considerable insight into the mechanism for the activation of TIM towards deprotonation of glycolaldehyde by phosphite dianion.

Kinetic studies show that substrate binding is largely rate-determining for k_{cat}/K_m in the TIM-catalyzed isomerization of GAP to give DHAP [24], and that product release is largely rate-determining for k_{cat} in the turnover of DHAP to give GAP [25]. The loop-open and loop-closed forms of TIM have been characterized by solid state [26-28] and solution [29,30] NMR spectroscopy, along with laser induced temperature jump fluorescence spectroscopy [31••]. These studies show that the rate constant for loop opening is similar to both k_{cat} for turnover of triosephosphates and the rate constants for release of enzyme-bound DHAP and GAP. This work has also shown that the motion of loop 6 associated with loop

opening, which occurs on the microsecond timescale, is similar for the free and liganded forms of TIM [26,30,31].

Loop Closure: Sequestration of Substrate from Solvent

The large activation of TIM, OMPDC and GPDH by HPO_3^{2-} towards catalysis of the reaction of truncated substrates requires, formally, that interactions between the enzyme and phosphite dianion be utilized in transition state stabilization. This activation is both a general consequence of the effect of loop closure on the *medium* in which the reaction is catalyzed, and a specific consequence of exquisitely orchestrated changes in the position of amino acid side chains during the conformational changes effected by the substrate phosphodianion group or phosphite dianion.

Studies of partitioning of the enediolate intermediate of the TIM-catalyzed reactions of GAP [32,33] and DHAP [34] in D_2O provide direct evidence that this intermediate is sequestered from bulk solvent. X-ray crystallography shows that closure TIM loop 6 over the substrate phosphodianion embeds the ligand within the protein (Figure 3). This leads to additional contacts between the protein and the substrate [2,3], and effectively transfers the substrate from water to a protein environment. The result is a decrease in the effective dielectric constant D_{eff} of the reaction medium, from the large value of 79 for water to perhaps as low as ca. 20 characteristic of the interior of proteins [35,36]. This in turn will have the effect of increasing the stabilizing coulombic interactions between the enzyme and ligands, which depend upon $1/D_{eff}$.

Highly conserved cationic amino acid side chains situated adjacent to the phosphate gripper loops of both TIM (Lys-12) [7,37] and OMPDC (Arg-235) [18] interact directly with the substrate phosphodianion group. The K12G mutation at TIM [8] and the R235A mutation at OMPDC [38,39•] result in 6×10^5-fold and 2×10^4 -fold decreases in k_{cat}/K_m for the enzyme-catalyzed isomerization of GAP and decarboxylation of OMP, respectively. This corresponds to 7.8 kcal/mol and 5.8 kcal/mol stabilizing interactions between the cationic side chain and the transition states for the wildtype enzyme-catalyzed reactions. These interactions are much stronger than the corresponding interactions of free cations with phosphodianions in aqueous solution [40,41]. This is the expected result if loop closure reduces the “effective” dielectric constant of medium and enhances electrostatic interactions between the cationic amino acid side chain and the phosphodianion group in the transition state.

An examination of the X-ray crystal stuctures for the wildtype enzymes shows that the K12G mutation at TIM and the R235A mutation at OMPDC should expose the phosphodianion group of the respective bound substrates to solvent. The binding of the guanidinium cation to R235A mutant OMPDC [39] and the binding of alkylammonium cations to K12G mutant TIM [42] restores to these mutants a substantial fraction of the wildtype enzyme activity. These studies provide estimates of the entropic advantage to the covalent attachment of the respective cationic activators to TIM and to OMPDC [39,42].

Loop Closure: Entropy Effects

Figure 4 shows the three sections of the highly conserved flexible loop 6 of TIM. X-ray crystal structures of the open and closed forms of TIM show that residues 169 – 173 (AIGTG) resemble a *tip* and move as a rigid body. The loop flexibility is apparently limited to the three-residue each N-terminal and C-terminal hinge regions [43]. This ensures rapid opening and closing of the loop, while minimizing the entropic cost of immobilizing the *tip* residues at the closed enzyme.

The codons for the [PVW] N-terminal hinge of chicken TIM have been replaced with a library of all possible 8,000 amino acid combinations, and the activity of the library of expressed proteins was analyzed [44]. Glycine peptide bonds are the most flexible of all peptide bonds. Therefore, the observation that only three of the active hinge mutants contained even a single glycine residue [44] suggests that there is an inverse relationship between catalytic activity and hinge flexibility.

A TIM mutant in which five of the six hinge residues (Figure 4) were replaced by glycine to give the loop sequence PGG-AIGTG-GGG shows a 2500-fold decrease in k_{cat} and a 10-fold increase in K_m compared to wildtype TIM [46]. NMR studies showed that this loop 6 mutant exhibits a greater conformational heterogeneity, but with motional rates for loop 6 that are an order of magnitude slower than for the natural loop motion of wildtype TIM [47•]. By contrast, loop motions on the nanosecond timescale are enhanced relative to wildtype TIM [47]. These data suggest that loop 6 has evolved to minimize the decrease in conformational entropy associated with loop closure [46], so that the large decrease in k_{cat}/K_m for the PGG-AIGTG-GGG double hinge mutant is partly or entirely due to the larger entropy of activation associated with the “freezing” of conformational motions of the unconstrained loop for the *open* enzyme on moving to the rigid loop at the closed enzyme [47].

Cooperativity in Loop Closure

The closure of loops 6 and 7 of TIM over the bound enediolate intermediate analog PGH is “driven” by the formation of a stunning array of hydrogen bonds (Figure 5) including: (A) Inter-loop H-bonds between: (i) the backbone amide NH of Gly-173 and the γ-O of Ser-211; (ii) the backbone amide NH of Ala-176 and the phenol oxygen of Try-208; and (iii) the carbonyl oxygen of Ala-169 and the γ-OH of Ser-211. (B) An intra-loop H-bond between the backbone amide NH of Gly-173 and the carbonyl oxygen of Ala-169 (not shown). (C) Hydrogen bonds between the phosphodianion group of PGH and the backbone amide NH groups of Gly-171 and Ser-211 [45,47,48]. There are additional hydrogen bonds between the ligand phosphodianion and the backbone amide NH groups of Gly-232 and Gly-233 in loop 8, whose strength may enhanced by the placement of these residues at the N-terminal end of a short α-helix that has the positive helix dipole directed toward the substrate phosphodianion group [4].

Disruption of this network of inter-loop hydrogen bonds impairs the TIM-catalyzed isomerization reaction. The Y208F mutation at yeast TIM eliminates the hydrogen bond with the amide NH of Ala-176 and it results in a 1000-fold decrease in k_{cat} for isomerization of GAP, a small 2-fold increase in K_m, and a 200-fold increase in K_i for inhibition by the intermediate analog PGH [48]. A dynamic NMR study of a Y208F TIM from chicken with no substrate bound showed an increase in the population of the open conformer that is consistent a ca. 0.8 kcal/mol increase in ΔG_o for conversion of the open to the closed conformer [49]. The stabilization of the open enzyme, which results in a decrease in the concentration of the active closed enzyme, can account for the 2-fold larger K_m for the mutant enzyme. The explanation for the large 1000-fold effect of the Y208F mutation on k_{cat} is not understood.

The YGGS motif at residues 208 - 211 of loop 7 of TIM is highly conserved but is replaced by other sequences in TIMs from archaebacteria [45]. The archaeal sequence of 208-TGAG has been substituted for the 208-YGGS sequence of wildtype TIM from chicken muscle [50•]. This replacement, which includes the Y208T mutation, causes only a 200-fold decrease in k_{cat}/K_m [50], which is *smaller* than the 2400-fold decrease reported for the Y208F point mutant [48]. These data show that the sterically conservative Y208F mutation has a larger unfavorable effect on catalytic activity than does the Y208T substitution, which conserves the polar OH group at the amino acid side chain.

Desolvation of Glu-165

There are six water molecules in the first solvation shell of acetate anion in water [51]. The X-ray crystal structure of unliganded TIM from *T. brucei* [52] reveals six water molecules within 5 Å of the side chain of the catalytic base Glu-167, so that this side chain is accessible to solvent. The closure of loop 6 over bound ligand occludes bulk solvent and displaces several water molecules from the active site. For example, only two waters lie within 5 Å of the side chain of Glu-167 at the complex between TIM from *Leishmania mexicana* and PGH [12].

Desolvation of the carboxylate anion side chain of the catalytic glutamate base at TIM and the low local dielectric constant of the active site cavity should lead to an increase in the basicity of this side chain over its basicity in solvent water. Indeed, there is good evidence that the binding of the intermediate analog PGA to TIM induces a 2.8 unit increase in the pK_a of the side chain of Glu-165 [53]. An atomic level X-ray crystal structure (0.82 Å resolution) of the enzyme•PGH complex for TIM from *L. mexicana* shows that the hydroxamate group of PGH interacts with Glu-167 via a seven-membered ring, with short hydrogen bond bridges running from the carboxylate oxygens of Glu-167 to N-1 (2.7 Å) and O-1 (2.6 Å) of the ligand (Figure 6) [12]. It was shown that formation of the yeast TIM•PGH complex produces two strongly deshielded ^{1}H NMR resonances at 14.9 and 10.9 ppm which were assigned to the N-O<u>H</u> and N-<u>H</u> of PGH, respectively [54]. The low H/D fractionation factor of $\Phi = 0.38$ for the resonance at 14.9 ppm shows that this proton lies in a low-barrier H-bond with the glutamate base [54], so that this weakly solvated carboxylate anion lies in a hydrophobic environment necessary for the formation of low-barrier hydrogen bonds [55]. X-ray [12] and ^{1}H NMR [54] structural analyses show that PGH is bound in the planar amidate form, which is a close analog of the enediolate reaction intermediate (Figure 6, inset).

A Hydrophobic Cage

The most important of the many motions that occur during the complex ligand-driven conformational change of TIM is the 2 Å shift of the active site base Glu-165 into its catalytically active position [10]. The shift in the position of Glu-165 is enabled by a 90° rotation of the Gly-209-Gly-210 peptide bond (numbering for chicken TIM) [45,56]. This is accompanied by a “flip” of the Gly-210-Ser-211 bond which allows the formation of a hydrogen bond between the backbone amide NH group of Ser-211 and the phosphodianion group of bound ligand [45,56]. The closure of loop 6 also causes the hydrophobic side chains of Ile-172 and Leu-232 (numbering for TIM from *T. brucei* or *L. mexicana*) to fold over the carboxylate side chain of Glu-167 [12,52,57•], where they act to shield both the ligand and the carboxylate base from interaction with bulk solvent. Figure 7A shows the complex between TIM (*T. brucei*) and glycerol 3-phosphate (G3P) [58], where the side chain of Glu-167 sits in a “hydrophobic cage” that is formed by the side chains of Ile-172 and Leu-232 and lined by Gly-211, Cys-126 and Ala-165 [12,52,57]. The ligand-driven movement of the side chain of Glu-167 into this structured hydrophobic environment will result in an increase in the basicity of the carboxylate anion that will promote deprotonation of enzyme-bound substrate.

Ile-172 is highly conserved in TIM sequences [45,57] and we have shown that the I172A mutation at TIM from *T. brucei* results in *decreases* of 350-fold in k_{cat} and 2-fold in K_m for the isomerization of GAP, along with a 40-fold increase in K_i for inhibition by the intermediate analog PGA [MM Malabanan, JP Richard, unpublished results]. Energy minimization of the liganded structure for I172A TIM created by *in silico* “mutation” [MM Malabanan, JP Richard, unpublished results] of the wildtype TIM•G3P complex [58] leads to positioning of the side chain of Glu-167 in the “swung-out” conformation that is

characteristic of unliganded wildtype TIM (Figure 7B) [52]. This suggests that the side chain of Glu-167 moves into the gap in the hydrophobic cage created by the I172A mutation.

The proline residue that follows the catalytic glutamate at the N-terminal of loop 6 (Figure 4) is conserved for over 100 TIMs [45]. The X-ray crystal structure of the complex between TIM (*L. mexicana*) and PGH shows that the pyrrolidine ring of Pro-168 adopts a strained planar conformation [56,57]. The results of a QM/MM computational study suggest that this strain is induced by interactions between the pyrrolidine ring and the side chains of Tyr-166 and Ala-171 [59]. The P168A mutation at TIM (*T. brucei*) results in *decreases* of ca. 50-fold in k_{cat} and 2-fold in K_m for the turnover of GAP and DHAP. X-ray crystallography showed that the P168A mutation causes the side chain of Glu-167 to move into the inactive "swung-out" position [56], in a fashion similar to that observed for the I172A mutant (Figure 7). Both the P168A and I172A mutations reduce the size of hydrophobic side chains at the enzyme active site and are accompanied by a shift in the position of the side chain of Glu-167. We speculate that steric crowding forces the desolvated side chain of Glu-167 into a "hydrophobic cage" where it lies very close to the carbon acid substrate and is *optimally aligned* to deprotonate bound substrate [9]. Mutations that relieve crowding are accompanied by a shift in the position of this side chain to a swung-out position that is distant from the substrate, and an associated loss in catalytic activity.

Concluding Remarks

There is a need to move from the enzyme-specific observations described in this review to a general model that rationalizes the observed phosphate/phosphite activation of enzyme-catalyzed proton transfer, hydride transfer and decarboxylation reactions (Chart 1). As a starting point, we suggest the model in Figure 8 [60]. This shows a dominant inactive open enzyme form (**E_o**), and a rare active closed enzyme form (**E_c**) which is stabilized by interactions of the phosphate gripper loop with bound HPO_3^{2-}. We propose that the free unliganded enzyme (**E_c**) and the HPO_3^{2-}-liganded enzyme (**E_c**•HPO_3^{2-}) in their *active closed* conformations exhibit similar reactivities in carbon deprotonation of the truncated substrate glycolaldehyde, so that $k_{cat}/K_m = (k_{cat}/K_m)'$ [16,60]. The intrinsic binding energy of HPO_3^{2-} is then utilized largely for the purpose of driving the unfavorable conformational change from **E_o** to give **E_c** [16,60]. This model predicts that the difference between the small *observed* free energy of binding of phosphite [$\Delta G_o = -RT\ln(K_c/K_{HPi})$, Figure 8] and the large *intrinsic* phosphite binding energy [$\Delta G_o = -RT\ln(1/K_{Pi})$] is the phosphite binding energy that is used specifically to drive the necessary, but thermodynamically unfavorable, conformational change from **E_o** to **E_c** [$\Delta G_o = -RT\ln K_c$]. Our current work is focused on understanding the specific mechanisms by which phosphite dianion drives loop closure and activates enzymes for catalysis of proton transfer, hydride transfer and decarboxylation reactions.

Acknowledgments

We acknowledge the NIH (GM39754) for generous support of our work described in this review.

REFERENCES

1. Koshland DE Jr. Application of a Theory of Enzyme Specificity to Protein Synthesis. Proc Natl Acad Sci, USA 1958;44:98–104. [PubMed: 16590179]
2. Herschlag D. The role of induced fit and conformational changes of enzymes in specificity and catalysis. Biorg Chem 1988;16:62–96.
3. Jencks WP. Binding energy, specificity, and enzymic catalysis: the Circe effect. Adv Enzymol Relat Areas Mol Biol 1975;43:219–410. [PubMed: 892]

4•. Knowles JR. To build an enzyme. Philos. Trans. R. Soc. London, Ser. B 1991;332:115–121. [PubMed: 1678530] [An excellent summary of our understanding in 1991 of the challenges faced by TIM in catalyzing deprotonation of weakly acidic carbon, and of the chemical strategies adopted by this enzyme]

5. Raines RT, Sutton EL, Straus DR, Gilbert W, Knowles JR. Reaction energetics of a mutant triose phosphate isomerase in which the active-site glutamate has been changed to aspartate. Biochemistry 1986;25:7142–7154. [PubMed: 2879556]

6. Komives EA, Chang LC, Lolis E, Tilton RF, Petsko GA, Knowles JR. Electrophilic catalysis in triosephosphate isomerase: the role of histidine-95. Biochemistry 1991;30:3011–3019. [PubMed: 2007138]

7. Lodi PJ, Chang LC, Knowles JR, Komives EA. Triosephosphate isomerase requires a positively charged active site: The role of lysine-12. Biochemistry 1994;33:2809–2814. [PubMed: 8130193]

8•. Go MK, Koudelka A, Amyes TL, Richard JP. The role of Lys-12 in catalysis by triosephosphate isomerase: A two-part substrate approach. Biochemistry 2010;49:5377–5389. [PubMed: 20481463] [Recently developed experimental protocols which characterize the partitioning of the enediolate intermediate are used to define the role of a critical amino acid side chains in TIM-catalyzed isomerization]

9. Jogl G, Rozovsky S, McDermott AE, Tong L. Optimal alignment for enzymatic proton transfer: structure of the Michaelis complex of triosephosphate isomerase at 1.2-Å resolution. Proc Natl Acad Sci, USA 2003;100:50–55. [PubMed: 12509510]

10. Lolis E, Petsko GA. Crystallographic analysis of the complex between triosephosphate isomerase and 2-phosphoglycolate at 2.5-Å resolution: implications for catalysis. Biochemistry 1990;29:6619–6625. [PubMed: 2204418]

11. Davenport RC, Bash PA, Seaton BA, Karplus M, Petsko GA, Ringe D. Structure of the triosephosphate isomerase-phosphoglycolohydroxamate complex: an analog of the intermediate on the reaction pathway. Biochemistry 1991;30:5821–5826. [PubMed: 2043623]

12••. Alahuhta M, Wierenga RK. Atomic Resolution crystallography of a complex of triosephosphate isomerase with a reaction intermediate analog: new insight in the proton transfer reaction mechanism. Proteins: Struct, Funct, Bioinf 2010;78:1878–1888. [An atomic level crystal structure of TIM complexed with an analog of the enediolate intermediate, which clearly defines the important enzyme-ligand interactions responsible for stabilization of the true reaction intermediate]

13. Zhang Z, Sugio S, Komives EA, Liu KD, Knowles JR, Petsko GA, Ringe D. Crystal structure of recombinant chicken triosephosphate isomerase-phosphoglycolohydroxamate complex at 1.8-Å resolution. Biochemistry 1994;33:2830–2837. [PubMed: 8130195]

14. Amyes TL, O'Donoghue AC, Richard JP. Contribution of phosphate intrinsic binding energy to the enzymatic rate acceleration for triosephosphate isomerase. J Am Chem Soc 2001;123:11325–11326. [PubMed: 11697989]

15. Richard JP. Acid-base catalysis of the elimination and isomerization reactions of triose phosphates. J Am Chem Soc 1984;106:4926–4936.

16. Amyes TL, Richard JP. Enzymatic catalysis of proton transfer at carbon: activation of triosephosphate isomerase by phosphite dianion. Biochemistry 2007;46:5841–5854. [PubMed: 17444661]

17. Banner DW, Bloomer AC, Petsko GA, Phillips DC, Wilson IA. Atomic coordinates for triose phosphate isomerase from chicken muscle. Biochem Biophys Res Comm 1976;72:146–155. [PubMed: 985462]

18. Miller BG, Hassell AM, Wolfenden R, Milburn MV, Short SA. Anatomy of a proficient enzyme: the structure of orotidine 5'-monophosphate decarboxylase in the presence and absence of a potential transition state analog. Proc Natl Acad Sci, USA 2000;97:2011–2016. [PubMed: 10681417]

19. Ou X, Ji C, Han X, Zhao X, Li X, Mao Y, Wong L-L, Bartlam M, Rao Z. Crystal structures of human glycerol 3-phosphate dehydrogenase 1 (GPD1). J Mol Biol 2006;357:858–869. [PubMed: 16460752]

20••. Tsang W-Y, Amyes TL, Richard JP. A substrate in pieces: Allosteric activation of glycerol 3-phosphate dehydrogenase (NAD+) by phosphite dianion. Biochemistry 2008;47:4575–4582. [PubMed: 18376850] [The most recent description of a two-part substrate protocol, which demonstrates the important role of enzyme-phosphite dianion interactions in activating the enzyme towards catalysis of the reaction of bound substrate]

21. Amyes TL, Richard JP, Tait JJ. Activation of orotidine 5'-monophosphate decarboxylase by phosphite dianion: The whole substrate is the sum of two parts. J Am Chem Soc 2005;127:15708–15709. [PubMed: 16277505]

22. Jencks WP. On the attribution and additivity of binding energies. Proc Natl Acad Sci, USA 1981;78:4046–4050. [PubMed: 16593049]

23. Morrow JR, Amyes TL, Richard JP. Phosphate binding energy and catalysis by small and large molecules. Acc Chem Res 2008;41:539–548. [PubMed: 18293941]

24. Blacklow SC, Raines RT, Lim WA, Zamore PD, Knowles JR. Triosephosphate isomerase catalysis is diffusion controlled. Biochemistry 1988;27:1158–1165. [PubMed: 3365378]

25. Knowles JR, Albery WJ. Perfection in enzyme catalysis: the energetics of triosephosphate isomerase. Acc Chem Res 1977;10:105–111.

26. Williams JC, McDermott AE. Dynamics of the flexible loop of triose-phosphate isomerase: The loop motion is not ligand gated. Biochemistry 1995;34:8309–8319. [PubMed: 7599123]

27. Rozovsky S, McDermott AE. The time scale of the catalytic loop motion in triosephosphate isomerase. J Mol Biol 2001;310:259–270. [PubMed: 11419951]

28. Xu Y, Lorieau J, McDermott AE. Triosephosphate isomerase: 15N and 13C chemical shift assignments and conformational change upon ligand binding by magic-angle spinning solid-state NMR spectroscopy. J Mol Biol 2010;397:233–248. [PubMed: 19854202]

29. Rozovsky S, Jogl G, Tong L, McDermott AE. Solution-state NMR investigations of triosephosphate isomerase active site loop motion: ligand release in relation to active site loop dynamics. J Mol Biol 2001;310:271–280. [PubMed: 11419952]

30. Massi F, Wang C, Palmer AG. Solution NMR and computer simulation studies of active site loop motion in triosephosphate isomerase. Biochemistry 2006;45:10787–10794. [PubMed: 16953564]

31••. Desamero R, Rozovsky S, Zhadin N, McDermott A, Callender R. Active site loop motion in triosephosphate isomerase: T-jump relaxation spectroscopy of thermal activation. Biochemistry 2003;42:2941–2951. [PubMed: 12627960] [The direct solution characterization of the rate constants for loop closure at TIM over the substrate analog glycerol 3-phosphate, and for loop opening to release bound ligand]

32. O'Donoghue AC, Amyes TL, Richard JP. Hydron transfer catalyzed by triosephosphate isomerase. Products of isomerization of (*R*)-glyceraldehyde 3-phosphate in D2O. Biochemistry 2005;44:2610–2621. [PubMed: 15709774]

33. O'Donoghue AC, Amyes TL, Richard JP. Slow proton transfer from the hydrogen-labelled carboxylic acid side chain (Glu-165) of triosephosphate isomerase to imidazole buffer in D2O. Org Biomol Chem 2008;6:391–396. [PubMed: 18175010]

34. O'Donoghue AC, Amyes TL, Richard JP. Hydron transfer catalyzed by triosephosphate isomerase. Products of isomerization of dihydroxyacetone phosphate in D2O. Biochemistry 2005;44:2622–2631. [PubMed: 15709775]

35. Teixeira VH, Cunha CA, Machuqueiro M, Oliveira ASF, Victor BL, Soares CM, Baptista AM. On the use of different dielectric constants for computing individual and pairwise terms in Poisson-Boltzmann studies of protein ionization equilibrium. J Phys Chem B 2005;109:14691–14706. [PubMed: 16852854]

36. Schutz CN, Warshel A. What are the dielectric “constants” of proteins and how to validate electrostatic models? Proteins: Struct, Funct, Genet 2001;44:400–417. [PubMed: 11484218]

37. Joseph-McCarthy D, Lolis E, Komives EA, Petsko GA. Crystal structure of the K12M/G15A triosephosphate isomerase double mutant and electrostatic analysis of the active site. Biochemistry 1994;33:2815–2823. [PubMed: 8130194]

38. Miller BG, Snider MJ, Short SA, Wolfenden R. Contribution of enzyme-phosphoribosyl contacts to catalysis by orotidine 5'-phosphate decarboxylase. Biochemistry 2000;39:8113–8118. [PubMed: 10889016]

39•. Barnett SA, Amyes TL, McKay Wood B, Gerlt JA, Richard JP. Activation of R235A mutant orotidine 5-monophosphate decarboxylase by the guanidinium cation: Effective molarity of the cationic side chain of Arg-235. Biochemistry 2010;49:824–826. [PubMed: 20050635] [A comparison of the stabilization of the transition state for OMPDC-catalyzed decarboxylation by the cationic side chain of Arg-235 in an effectively intramolecular reaction of wildtype enzyme, and by the guanidinium cation in the intermolecular activation of the decarboxylation reaction catalyzed by R235A mutant OMPDC]

40. Haake P, Prigodich RV. Method for determination of phosphate anion-cation association constants from phosphorus-31 chemical shifts. Inorg Chem 1984;23:457–462.

41. Springs B, Haake P. Equilibrium constants for association of guanidinium and ammonium ions with oxyanions. Biorg Chem 1977;6:181–190.

42. Go MK, Amyes TL, Richard JP. Rescue of K12G triosphosphate isomerase by NH4+ and primary alkylammonium cations: The reaction of an enzyme in pieces. J Am Chem Soc 2010;132 ASAP, **DOI:**10.1021/ja106104h.

43. Joseph D, Petsko GA, Karplus M. Anatomy of a conformational change: hinged “lid” motion of the triosephosphate isomerase loop. Science 1990;249:1425–1428. [PubMed: 2402636]

44. Sun J, Sampson NS. Determination of the amino acid requirements for a protein hinge in triosephosphate isomerase. Protein Sci 1998;7:1495–1505. [PubMed: 9684881]

45. Kursula I, Salin M, Sun J, Norledge BV, Haapalainen AM, Sampson NS, Wierenga RK. Understanding protein lids: structural analysis of active hinge mutants in triosephosphate isomerase. Protein Eng Des Sel 2004;17:375–382. [PubMed: 15166315]

46. Xiang J, Jung J-Y, Sampson NS. Entropy effects on protein hinges: The reaction catalyzed by triosephosphate isomerase. Biochemistry 2004;43:11436–11445. [PubMed: 15350130]

47•. Kempf JG, Jung J-Y, Ragain C, Sampson NS, Loria JP. Dynamic requirements for a functional protein hinge. J Mol Biol 2007;368:131–149. [PubMed: 17336327] [Dynamic NMR studies which provide clear evidence that a degree of structrual rigidity in loop 6 of TIM is required for the observation of rapid opening and closing of the loop over enzyme-bound substrate]

48. Sampson NS, Knowles JR. Segmental motion in catalysis: investigation of a hydrogen bond critical for loop closure in the reaction of triosephosphate isomerase. Biochemistry 1992;31:8488–8494. [PubMed: 1390633]

49. Berlow RB, Igumenova TI, Loria JP. Value of a hydrogen bond in triosephosphate isomerase loop motion. Biochemistry 2007;46:6001–6010. [PubMed: 17455914]

50•. Wang Y, Berlow R, Loria J. Role of loop-loop interactions in coordinating motions and enzymatic function in triosephosphate isomerase. Biochemistry 2009;48:4548–4556. [PubMed: 19348462] [The latest in a series of sophisticated dynamic NMR studies that define the role of loop motion in TIM-catalyzed isomerization]

51. Alagona G, Ghio C, Kollman P. Monte Carlo simulation studies of the solvation of ions. 1. Acetate anion and methylammonium cation. J Am Chem Soc 1986;108:185–191.

52. Wierenga RK, Noble MEM, Vriend G, Nauche S, Hol WGJ. Refined 1.83 Å structure of trypanosomal triosephosphate isomerase crystallized in the presence of 2.4 M-ammonium sulfate. A comparison with the structure of the trypanosomal triosephosphate isomerase-glycerol-3-phosphate complex. J Mol Biol 1991;220:995–1015. [PubMed: 1880808]

53. Richard JP. The enhancement of enzymatic rate accelerations by Bronsted acid-base catalysis. Biochemistry 1998;37:4305–4309. [PubMed: 9556344]

54. Harris TK, Abeygunawardana C, Mildvan AS. NMR studies of the role of hydrogen bonding in the mechanism of triosephosphate isomerase. Biochemistry 1997;36:14661–14675. [PubMed: 9398185]

55. Chen J, McAllister MA, Lee JK, Houk KN. Short, strong hydrogen bonds in the gas phase and in solution: Theoretical exploration of pK_a matching and environmental effects on the strengths of hydrogen bonds and their potential roles in enzymic catalysis. J Org Chem 1998;63:4611–4619.

56. Casteleijn MG, Alahuhta M, Groebel K, El-Sayed I, Augustyns K, Lambeir AM, Neubauer P, Wierenga RK. Functional role of the conserved active site proline of triosephosphate isomerase. Biochemistry 2006;45:15483–15494. [PubMed: 17176070]

57•. Kursula I, Wierenga RK. Crystal structure of triosephosphate isomerase complexed with 2-phosphoglycolate at 0.83-Å resolution. J Biol Chem 2003;278:9544–9551. [PubMed: 12522213] [A particularly perceptive analysis of an atomic level structure of TIM liganded with 2-phosphoglycolate which provides new insight into the catalytic mechanism]

58. Noble MEM, Wierenga RK, Lambeir AM, Opperdoes FR, Thunnissen AMWH, Kalk KH, Groendijk H, Hol WGJ. The adaptability of the active site of trypanosomal triosephosphate isomerase as observed in the crystal structures of three different complexes. Proteins: Struct, Funct, Genet 1991;10:50–69. [PubMed: 2062828]

59. Donnini S, Groenhof G, Wierenga RK, Juffer AH. The planar conformation of a strained proline ring: a QM/MM study. Proteins 2006;64:700–710. [PubMed: 16741995]

60. Go MK, Amyes TL, Richard JP. Hydron transfer catalyzed by triosephosphate isomerase. Products of the direct and phosphite-activated isomerization of [1-13C]-glycolaldehyde in D2O. Biochemistry 2009;48:5769–5778. [PubMed: 19425580]

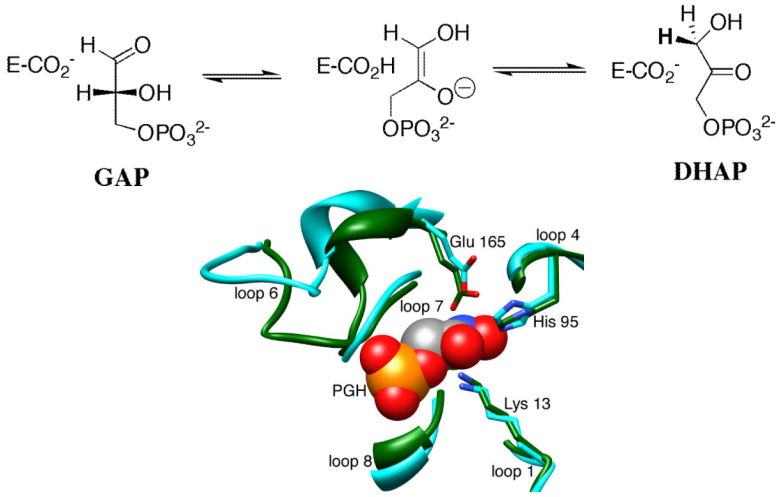

Figure 1.

(A) The isomerization of GAP to DHAP catalyzed by TIM, which proceeds by a proton transfer mechanism through an enediolate intermediate [4,8]. (B) The crystal structures of the loop-open and loop-closed forms of TIM from chicken muscle. The aqua ribbons are for the open unliganded enzyme [PDB entry 1TIM] [17] and the green ribbons show the closed enzyme liganded with 2-phosphoglycolohydroxamate (PGH) [PDB entry 1TPH] [13].

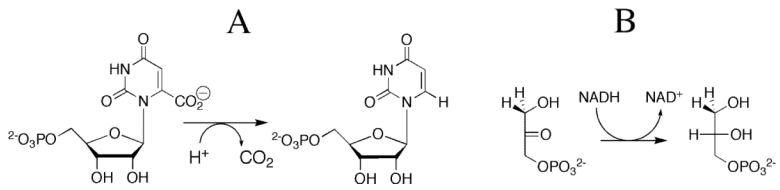

Figure 2.
(A) Decarboxylation reaction catalyzed by orotidine 5'-monophosphate decarboxylase. (B) Hydride transfer reaction catalyzed by glycerol 3-phosphate dehydrogenase.

Enzymatic Reaction	Natural Substrate	$(k_{cat}/K_m)_{SPi}$ M^{-1} s^{-1}	Truncated Substrate	$(k_{cat}/K_m)_S$ M^{-1} s^{-1}	Phosphate IBE	Substrate Piece	$(k_{cat}/K_m)_S/K_d$ M^{-2} s^{-1}	Phosphite IBE
Decarboxylation [21] OMP $\xrightarrow{\text{OMPDC}}$ UMP (CO_2)	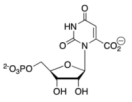	9.4×10^6	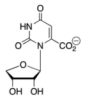	0.021	-11.8 kcal/mol	HPO_3^{2-}	12,000	-7.8 kcal/mol
Proton Transfer [16] GAP $\xrightarrow{\text{TIM}}$ DHAP		2.4×10^8		0.26	-12.2 kcal/mol	HPO_3^{2-}	4900	-5.8 kcal/mol
Hydride Transfer [20] DHAP $\xrightarrow{\text{GPDH}}$ α-GP (E•NADH → E•NAD$^+$)		1.0×10^6		0.0087	≤ -11.0 kcal/mol	HPO_3^{2-}	4300	-7.7 kcal/mol

Chart 1.

A comparison of the intrinsic binding energies (IBEs) of the substrate phosphodianion group and the phosphite dianion piece for the reactions catalyzed by OMPDC, TIM, and GPDH. The IBE for the substrate phosphodianion is calculated from the ratio of the second-order rate constants for turnover of the whole $[(k_{cat}/K_m)_{SPi}]$ and the truncated $[(k_{cat}/K_m)_S]$ substrates. The IBE for phosphite dianion is calculated from the ratio of the third-order rate constant for the phosphite-activated turnover of the truncated substrate $[(k_{cat}/K_m)_S/K_d]$ and the second-order rate constant for turnover of the truncated substrate $[(k_{cat}/K_m)_S]$.

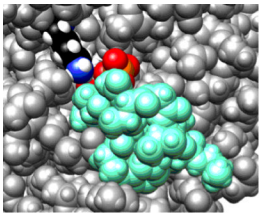

Figure 3.
Space-filling model of the surface of yeast TIM, with DHAP bound, in the region of the active site [PDB entry 1NEY] [9]. The flexible loop 6 is colored cyan, the alkylammonium side chain of Lys-12 is colored black (C), white (H) and blue (N). The visible part of the bound substrate is colored red (O) and orange (P).

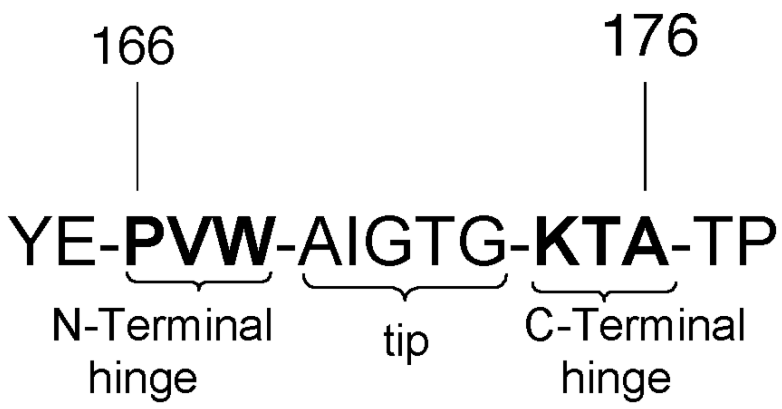

Figure 4.
The highly conserved [44,45] sequence of loop 6 of TIM from chicken muscle.

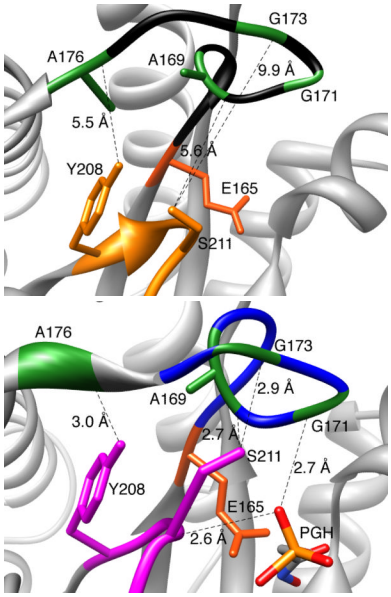

Figure 5.

A comparison of the *relaxed* open form and the *tightened* closed form of TIM from chicken muscle showing the formation of important inter-loop interactions upon ligand binding. (A) The active site of the unliganded open conformation [PDB entry 1TIM] [17]. (B) The active site of TIM liganded with PGH [PDB entry 1TPH] [13], an analog of the enediolate intermediate [12].

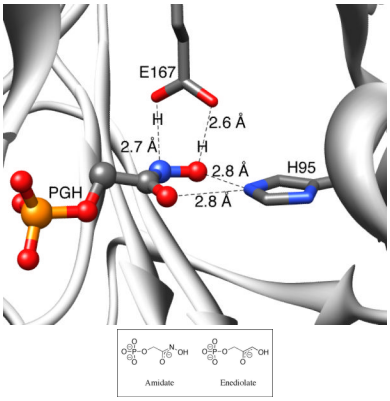

Figure 6.

The 0.82 Å resolution structure of the complex between TIM (*L. mexicana*) and the enediolate intermediate analog PGH [PDB entry 2VXN] [12]. PGH is bound in the planar amidate form [12,54] and it was suggested that the N-H of PGH lies closest to the carboxylate oxygen [12]. The distances from N-2 of His-95 to O-1 (2.8 Å) and O-2 (2.8 Å) of PGH are as expected for normal hydrogen bonds [12]. The inset compares the structures of the amidate form of PGH and the enediolate intermediate of the TIM-catalyzed isomerization reaction.

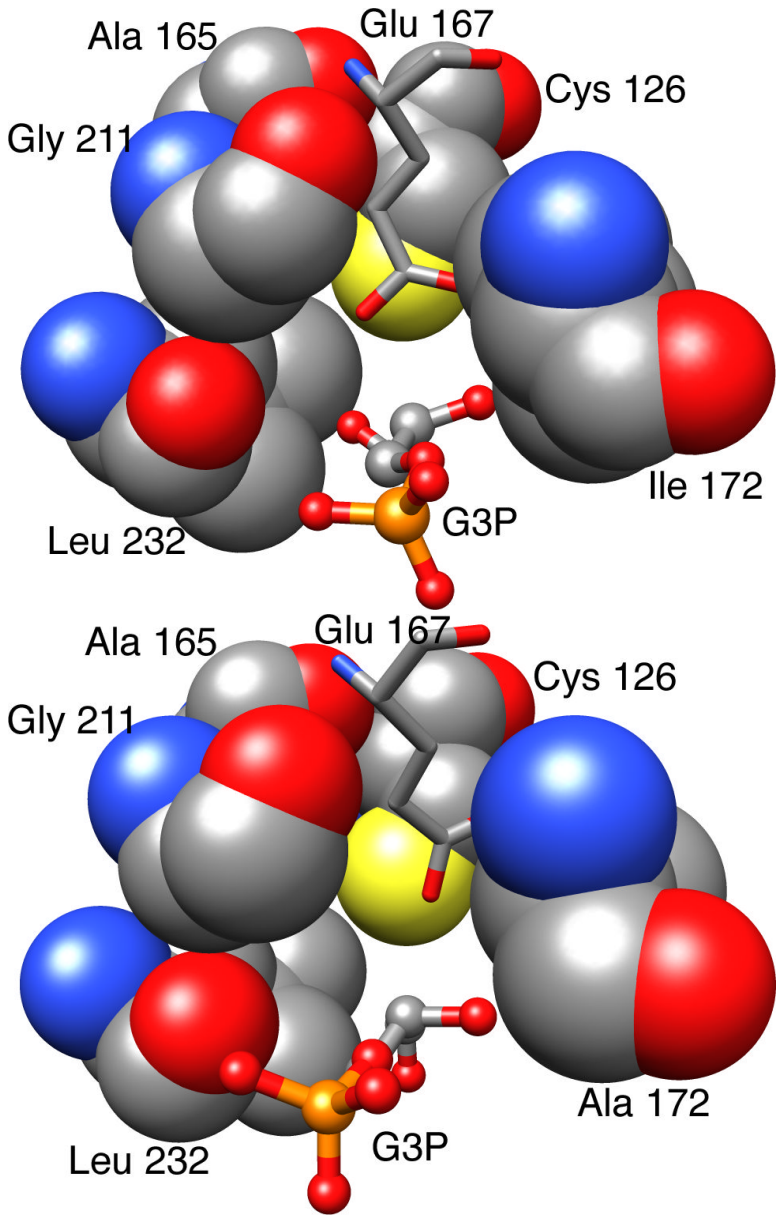

Figure 7.

(A) The structure of the complex between TIM (*T. brucei*) and glycerol 3-phosphate (G3P) [PDB entry 6TIM] [58]. The side chain of Glu-167 sits in a “hydrophobic cage”. (B) The structure of I172A mutant TIM (*T. brucei*) complexed with G3P, prepared starting with the coordinates for the wildtype enzyme complexed with G3P [PDB entry 6TIM] [58] and using the molecular graphics software SYBYL version 7.3 (Tripos Inc., St. Louis, MO).

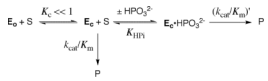

Figure 8.

A model developed to rationalize the observation that the binding of HPO_3^{2-} activates enzymes that utilize a flexible phosphate gripper loop for catalysis of the reaction of a truncated substrate S [20]. The enzyme is shown to exist in an inactive loop-open form (**E_o**) and a rare active loop-closed form (**E_c**) that is stabilized by the binding of HPO_3^{2-} [16,60].